

# **SEDIMENTOLOGICAL AND COMPOSITIONAL STUDIES OF ITORI WELL, EASTERN DAHOMEY BASIN, SOUTHWESTERN NIGERIA**

Nton, M.E<sup>1</sup>, \*Adesanoye, T.P<sup>1</sup>, Omotayo, J.O<sup>1</sup> and Omietimi, E.J<sup>2</sup>

<sup>1</sup>Department of Geology, University of Ibadan, Ibadan, Nigeria  
ntonme@yahoo.com; adesanoyetemitopepaul@gmail.com  
omotayojuliana1997@gmail.com

<sup>2</sup>Department of Geology, University of Pretoria, South Africa  
erepamo.omietimi@tuks.co.za

Sedimentological and compositional studies were carried out on subsurface samples of Itori well, within the eastern Dahomey basin to determine the lithofacies association, provenance, tectonic setting and depositional environment. The well interval of 55-320m consisting of eighteen (18) limestone and two (2) sandstone samples used for this study were subjected to sedimentological description, thin section petrography and geochemical analyses entailing major elemental oxides, trace elements as well as rare earths element were conducted using X- ray refraction method (XRF) and inductively Coupled Plasma-Mass Spectroscopy (ICP-MS) respectively.

The sandstone is classified as Quartz Arenite, while the limestone revealed two microfacies, Sandy bioclastic packstone and Bioclastic wackstone-packstone. The major oxides composition of the sandstone revealed SiO<sub>2</sub>, Al<sub>2</sub>O<sub>3</sub>, Fe<sub>2</sub>O<sub>3</sub>, TiO<sub>2</sub> and CaO constituting about 95wt%, oxides such as; MgO, Na<sub>2</sub>O, K<sub>2</sub>O, V<sub>2</sub>O<sub>3</sub>, MnO, NiO, ZrO<sub>2</sub>, ZnO and SrO are < 1 wt % each. The limestone reveals that; SiO<sub>2</sub>, Al<sub>2</sub>O<sub>3</sub>, Fe<sub>2</sub>O<sub>3</sub>, TiO<sub>2</sub> and CaO constitute about 90% wt %, oxides such as MgO, Na<sub>2</sub>O, K<sub>2</sub>O, V<sub>2</sub>O<sub>3</sub>, ZnO and SrO are < 1wt. % each. Ti, P and Sr dominated the trace element suites. The Th/Sc, Th/Co Th/Cr and Cr/Th ratios of the sediments suggested intermediate to felsic provenance, Cross plot of K<sub>2</sub>O/Na<sub>2</sub>O vs SiO<sub>2</sub> revealed Active and Passive Continental Margin tectonic setting while bivariate plot of SiO<sub>2</sub> against total (Al<sub>2</sub>O<sub>3</sub> + K<sub>2</sub>O + Na<sub>2</sub>O) revealed the prevalence of semi-humid conditions for the sediments. The V/Cr, P/Ti, Zr/Rb and Sr/Ba ratios suggested oxic condition, high productivity, strong hydrodynamic conditions and high salinity respectively at the time of deposition of sediments. It can be deduced that the sandstone is a product of recycled nearby basement rocks, under passive and active continental margins with low weathering conditions while the limestone is of shallow marine origin with terrigenous influx.

## 1.0 Introduction

The Dahomey Basin is an extensive sedimentary basin on the continental margin of the Gulf of Guinea which extends from the Volta Delta in Ghana in the west to the Okitipupa Ridge in Nigeria in the east (Whiteman, 1982) (Fig.1). The distance from the Volta delta to the axis of the Okitipupa Ridge or Ilesha spur is about 440km and the width of the basin measured from the northern onshore margin in Benin (Dahomey) to the 3,000m bathymetric contour is about 224km (Whiteman, 1982). The area of the onshore part of the Dahomey Basin in all four countries involved (Ghana, Togo, Benin and Nigeria) up to the shelf break, probably does not exceed 30,400sq.km (Whiteman, 1982). The basin contains extensive wedge of Cretaceous to Recent sediments up to 3000m, which thickens from the onshore margin

Various aspects of the geology of the eastern Dahomey basin have also been discussed, viz: stratigraphy (Fayose. 1970; Ogbe, 1972; Omatsola and Adegoke. 1981); sedimentology (Elueze and Nton, 2004; Nton and Elueze, 2005) and hydrocarbon source potential (Nwachukwu and Adedayo, 1987; Ekweozor and Nwachukwu, 1989; Ekweozor, 1990; Elueze and Nton, 2004; Nton *et al.*, 2009) among others. Nton *et al.* (2009), also conducted some Rock-eval studies of Maastrichtian-Paleocene shales and limestones within the offshore Dahomey Basin and reported that the organic matter is low to adequate of terrestrial origin, immature to slightly mature, with prospect to generate gas rather than oil at appropriate maturity. The eastern Dahomey basin has proved to be of great geological interest, particularly because of occurrences of limestone, phosphate, glass sands and bitumen.

It has been reported that the chemical composition of clastic sedimentary rocks is a function of a complex interplay of several variables, including the nature of source rocks, source area weathering and diagenesis (Bhatia, 1983; Roser and Korsch, 1986; McLennan *et al.*, 1993). However, the tectonic setting of the sedimentary basins has been considered as the overall primary control on the composition of sedimentary rocks as different tectonic environments have distinctive provenance characteristics and also distinctive sedimentary processes (Dickinson, 1985; Shiloh *et al.* 2006).

The present study therefore integrates sedimentological and inorganic geochemical signatures of Itori Well sediments in the eastern Dahomey Basin, in predicting the provenance, tectonic settings, as well as palaeodepositional environment of the well. This study, no doubt will provide additional information that would be useful to researchers and explorationist as presently such information is scanty.

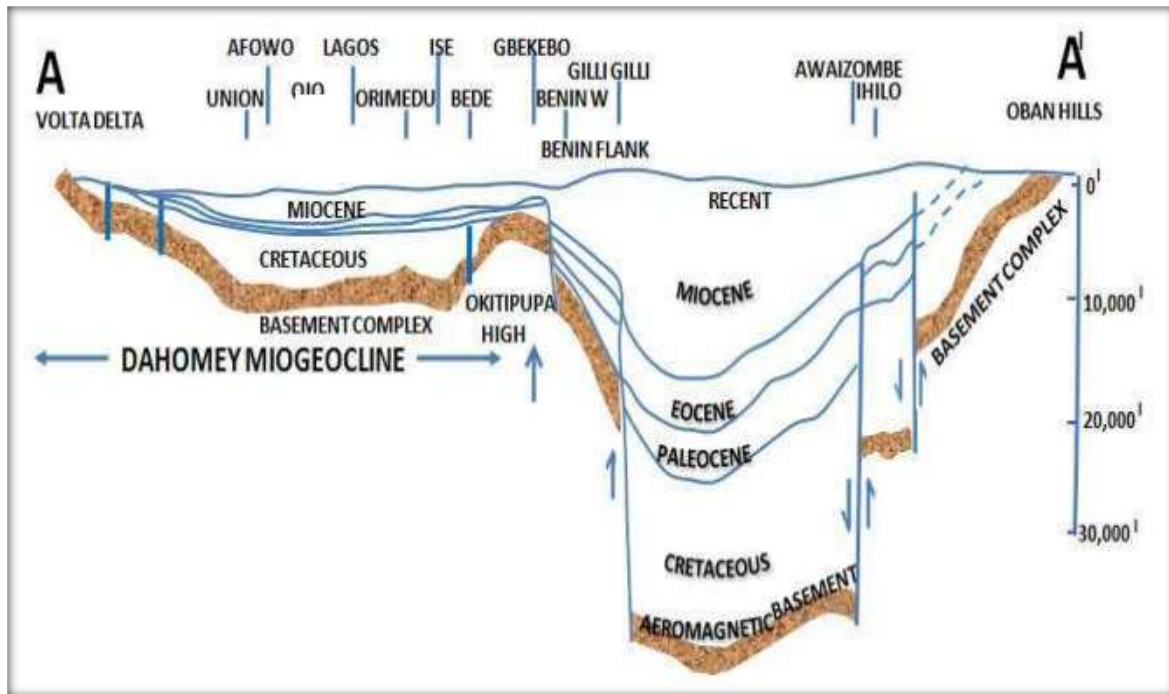


Fig. 1. East-West Geological section showing position, extent and sediment thickness variations in the onshore Dahomey Basin and the upper part of the Niger Delta (After Whiteman, 1982).

## Location of Study Area and Geology

The Itori Well, is located within the eastern Dahomey Basin, Southwestern Nigeria and lies within Latitude 7° 6' 0" N and Longitude 3° 25 ' 60 ". (Fig. 2). The stratigraphy of the eastern Dahomey Basin has been discussed by various workers; (Jones and Hockey, 1964; Reyment ,1965; Fayose, ,1970; Ogbe, 1972; Omatsola and Adegoke, 1981; Agagu, 1985; Billman, 1992; Nton, 2001; Elueze and Nton, 2004; Nton *et al.*, 2006) amongst others, and several classification schemes have been proposed (Omatsola and Adegoke, 1981; Billman, 1992; Ogbe, 1972,). However, controversies still exists in the classification schemes, age assignments, and terminologies of the different lithological units within this basin (Nton *et al*, 2009). Different stratigraphic names have been proposed for the same formation in different localities as a result of the lack of good borehole coverage and adequate outcrops for detailed stratigraphic studies (Billman, 1992; Okosun, 1990). Omatsola and Adegoke (1981), proposed the Cretaceous sequence in the eastern Dahomey Basin as beginning with the Abeokuta Group; The Abeokuta Group is the oldest sedimentary unit resting unconformably on the basement complex (Table 1) and made up of the Ise, Afowo and Araromi Formations successively. The Ise Formation is made up of grits and conglomerate at the base overlain by coarse-grained loose sands with intermediate kaolinite. Both the cross-bedding azimuth of the sandstone and the pebble alignments point to a NE palaeo-current system (Nton, 2001). According to Omatsola and Adegoke, (1981) a Neocomian (probably Valanginian – Barremian) age has been assigned to this formation based on palynomorphs. Overlying the Ise Formation is the Afowo Formation, which is composed mainly of coarse to medium-grained sandstone, with variable, thick interbedded shales, siltstones and clays; with the shale component increasing towards the top. The lower part consists of an alternation of brackish to marginal marine strata, with well-sorted, subrounded, clean, loose, fluviatile sands. Its maximum known thickness is 2,300m ( Omatsola and Adegoke, 1981) . The Afowo Formation is overlaid by the Araromi Formation, which comprised fine to medium – grained sands at base, and overlain by shale and siltstone with thin interbedded limestones and marls. This formation is the youngest of the Cretaceous sequences in the eastern Dahomey basin (Omatsola and Adegoke, 1981). Occurrences of thin lignitic bands are also common. The shales grade from light grey to black, and are mostly marine with a high organic content (Nton, 2001; Elueze and Nton; 2004). The Ewekoro Formation overlies the Araromi Formation and it is predominately limestone; the top is highly scoured and consists of red, dense, glauconitic, phosphatic and fossiliferous limestone. It is Palaeocene in age

and associated with shallow marine environment due to abundance of coralline algae, gastropods, pelecypods, echinoid fragment and other skeletal debris (Nton, 2001).

The Ewekoro Formation (where encountered) is overlain by predominantly shaley unit of the Akinbo Formation (Ogbe, 1972). The Akinbo Formation consists of dark micro micaceous, fine-textured shale that is locally silty with glauconitic marl and conglomerate at the base (Dessauvage, 1975). It consists of laminated and glauconitic shale and kaolinitic clay sequence (Nton and Elueze, 2005). The shales are grey, fissile, clayey and concretionary and dip gently ( $<5^{\circ}\text{SW}$ ) (Nton, 2001). The Oshosun Formation overlies the Akinbo Formation and consist of greenish- grey or beige clay and shale with interbeds of sandstone. The shale is thickly laminated and glauconitic. This formation is phosphate-bearing and is compositionally phosphorite (Nton, 2001). The Ilaro Formation overlies the Oshosun Formation in the eastern Dahomey basin, and consist of massive, yellow, poorly consolidated, cross bedded sandstone (Nton, 2001). The Benin Formation, is the youngest sedimentary unit in the eastern Dahomey basin and consist of a series of poorly sorted sands with lenses of clays and are in parts cross bedded (Agagu, 1985).

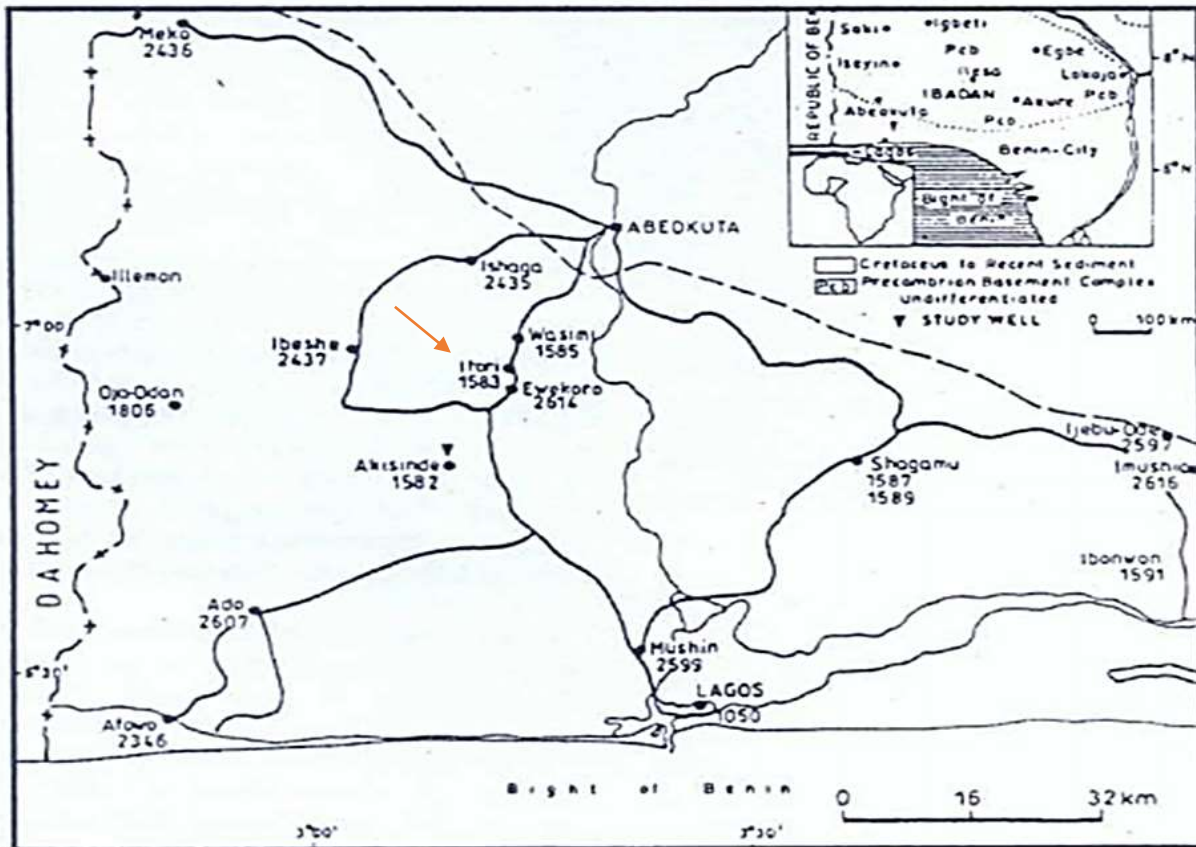


Fig 2: Location of some boreholes in eastern Dahomey Basin (modified after Jones and Honey, 1964).

Table 1: Cretaceous and Tertiary Stratigraphy of Nigeria part of Dahomey Basin (Olabode, 2006).

AGE		GROUP	FORMATIONS
QUATERNARY			BENIN (COASTAL PLAIN SANDS)
TERTIARY	PLIOCENE		ILARO
	MIOCENE		
	OLIGOCENE		
	EOCENE		
	PALEOCENE		
CRETACEOUS	MAASTRICHTIAN		ARAROMI
	CAMPANIAN	AFOWO	
	SANTONIAN		
	CONIACIAN		
	TURONIAN	ISE	
	CENOMANIAN		
	ALBIAN		
	APTIAN		
	BARREMIAN	OKITIPUPA RIDGE (BASEMENT)	
	NEOCOMIAN		



### **3.0 Material and method**

#### **3.1 Samples**

Subsurface samples of Itori well were obtained from the Nigeria Geological Survey Agency (NGSA), Kaduna, for this study. These samples were logged and taken in well –labeled sample bags to the Department of Geology, University of Ibadan for further examination and selection for laboratory analyses. In the Sedimentological Laboratory, the samples were described based on lithology, texture, color, sorting and fossil content, among others using a handlens. A total of twenty (20) representative sample from depth ranging from 55m to 320m, were selected for subsequent analyses.

#### **Thin Section petrography**

A total of twenty (20) representative samples were selected for thin section petrography. Since the samples were loosely consolidated, they were impregnated with resin before cutting. Each sample was mounted on a glass slide using Canada balsam by standard preparation methods and later examined under the petrology microscope stereo series model Meiji technology. Point count method was used for the mineral count and the individual percentages of the mineral were computed. Photomicrographs of features of interest were also taken.

#### **Geochemical Analyses**

##### **Major Oxides**

Twelve (12) samples were selected for geochemical analysis. The samples were first pulverized and about 2-3 grams of each was weighed out using a sensitive electrical digital weighing balance for analyses. Each pulverized samples was taken into a sample cup and analyzed for their major oxides. The samples were dried and roasted in alumina refractory crucibles, @ 100°C and 1000°C respectively, to determine Loss on Ignition (LOI). 1g of each sample was mixed with 6g Lithiumtetraborate flux and fused at 1030°C to make a stable fused glass bead.

The Thermo Fisher ARL Perform'X Sequential XRF instrument with Uniquant software, was used for the analysis. The values were normalized, to include LOI, to determine crystal water and oxidation state changes. A standard sample material was prepared and analyzed in the same

manner as the samples and reported as such. The XRF analysis was carried out at Stoneman's Laboratory, Department of Geology, University of Pretoria, South Africa.

### **Trace and Rare elements**

Twenty (12) samples were used for minor and REE geochemical analysis (electronic supplementary material 1). Circa 7–10 g of each sample, pulverized to  $<75\ \mu\text{m}$  in a Tungsten Carbide milling vessel, was roasted at  $1000\ ^\circ\text{C}$  to determine Loss on ignition (LOI), and fused into a glass bead. Aliquot of the sample was pressed into a powder briquette to determine trace elements. Preparation of samples and analyses were carried out using standard methods after Loubser and Verryin (2008). Analyses of trace elements and REE were conducted using a Thermo Scientific iCAPRQ for inductively coupled plasma mass spectrometry (ICP-MS) at the Earth Lab, University of Witwatersrand, South Africa.

## **Results and Discussions**

### **Lithological Description**

The lithologic succession of the well is shown in (Fig 3) and it is made up predominantly of sandy unit at base overlain by limestone sequence. The sandstone is sub rounded to well rounded, well sorted and fine grained. The overlying limestone unit is calcareous, greenish and highly fossiliferous. The well interval penetrated the topmost part of the Abeokuta Formation (Araromi Formation) which is the sandy base while the overlying limestone belongs to the Ewekoro Formation.

### **Petrography**

The result of sandstone petrography is shown in Table 2. The modal analysis shows that the dominant mineral in the sandstone sample is quartz (90-94%) with feldspar  $< 3.5\%$  and rock fragments content  $< 2\%$ . Other minor minerals include; Rutile, Garnet and Tourmaline. The feldspars are partly weathered and the rock fragments are mainly those of igneous and metamorphic varieties. The quartz grains are more of monocrystalline variety while the cementing material is silica, with optical continuity with the quartz grains. (Fig 4)

The sandstone sample is sub rounded to well rounded, well sorted and fine grained. and classified as Quartz Arenite (Fig. 5) The presence of garnet, tourmaline and rutile suggest igneous and metamorphic provenance of nearby basement complex (Table 2)

The modal composition of the limestone petrography is presented in Table 3. The limestone consists of skeletal and non-skeletal grains (Fig 6). The skeletal grains include broken shell fragments, some of which are preserved while others have been replaced by calcite spar (Fig. 6a). Ooids were abundant in many samples and were generally associated with bioclast surrounded with micritic matrix. The presence of ooids and peloids are indications of low-energy, warm and shallow seas supersaturated with  $\text{CaCO}_3$  having restricted circulation (Akaegbobi and Ogungbesan, 2016).

Two generations of sparry calcite cementation were identified in the studied limestone; the first generation with relatively large, equant and blocky crystalline cements that filled pore spaces between allochems and also the internal space in allochems (Fig 6c). Which was interpreted to have been precipitated under meteoric phreatic-burial zone. The second generation cement are small equant and blocky crystalline cement that also filled spore space between allochem (Fig.6a). Limestone microfacies are made up of bioclastic packstone, and bioclastic wackstone-packstone.(Fig. 3).

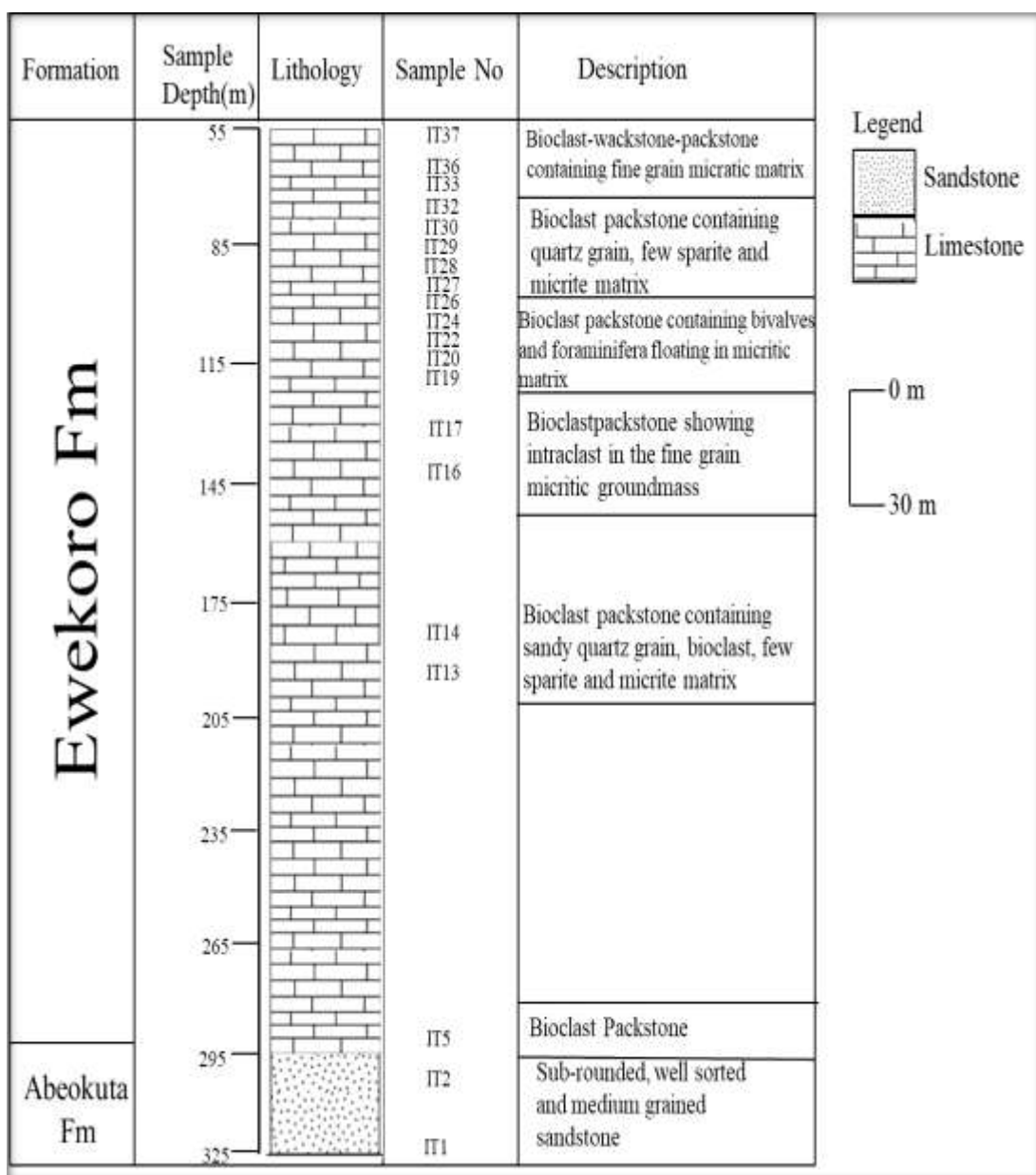


**Fig 3: Lithological section of Itori well**

**Table 2: Relative abundance of the constituents and framework composition of Itori well Sandstone.**

Sample no	Formation	Quartz (%)	Feldspar (%)	Rock fragment (%)	Other Minerals present (%)			Framework composition (%)	
					R	G	T	Q	F
IT 1	Abeokuta	93	3	2	1	-	1	94.89	3.06
IT2	Abeokuta	94	2	2	-	1	1	95.91	2.04

**R= Rutile T=Tourmaline G = Garnet**

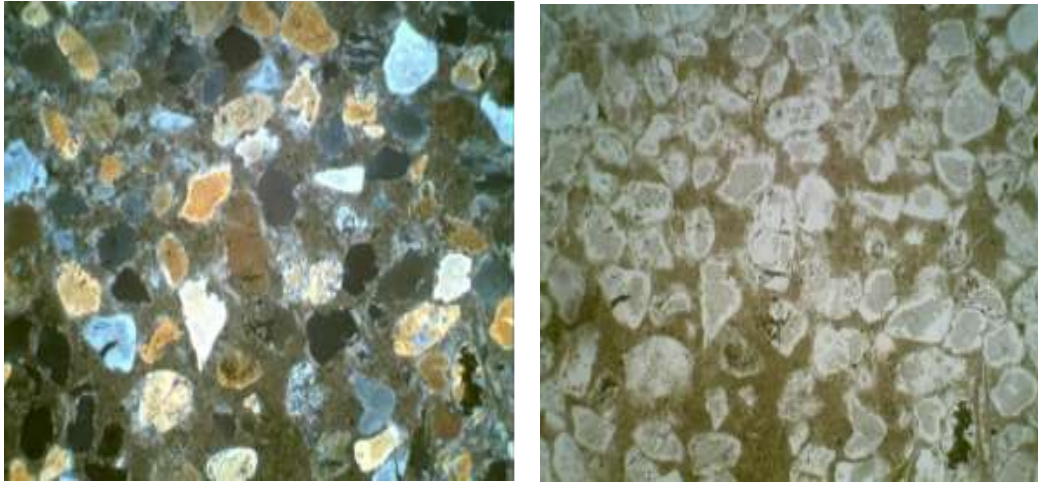


**Fig 4: Photomicrograph of Quartz Arenite of the Itori well (IT1) under XPL and PPL characterized by well sorted quartz grain (Mag =40x)**

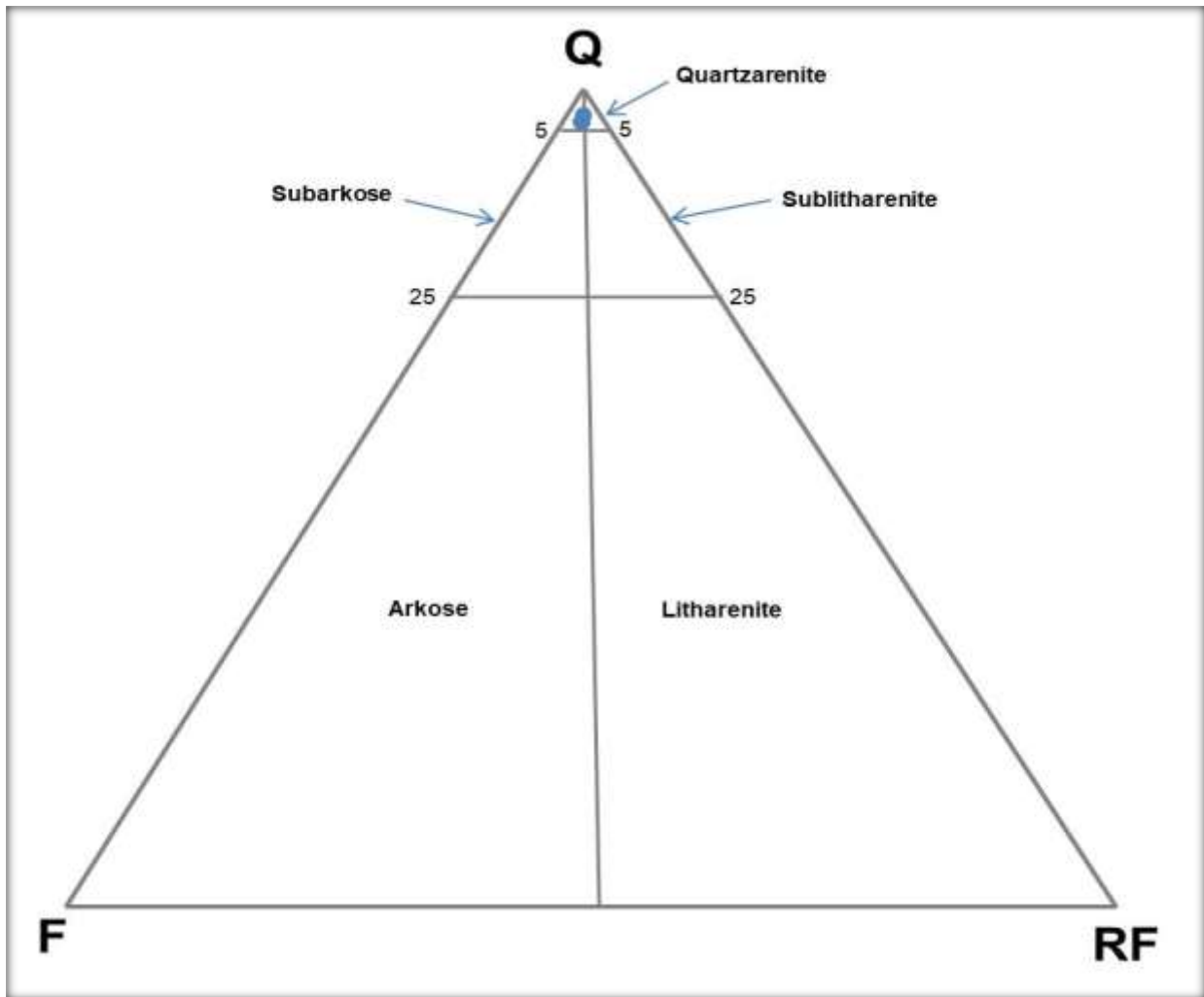


**Fig 5: Ternary Diagram for Classification of sandstone based on Framework composition (After: Folk 1974) Note: Q= Quartz, F= Feldspar, RF= Rock Fragment**

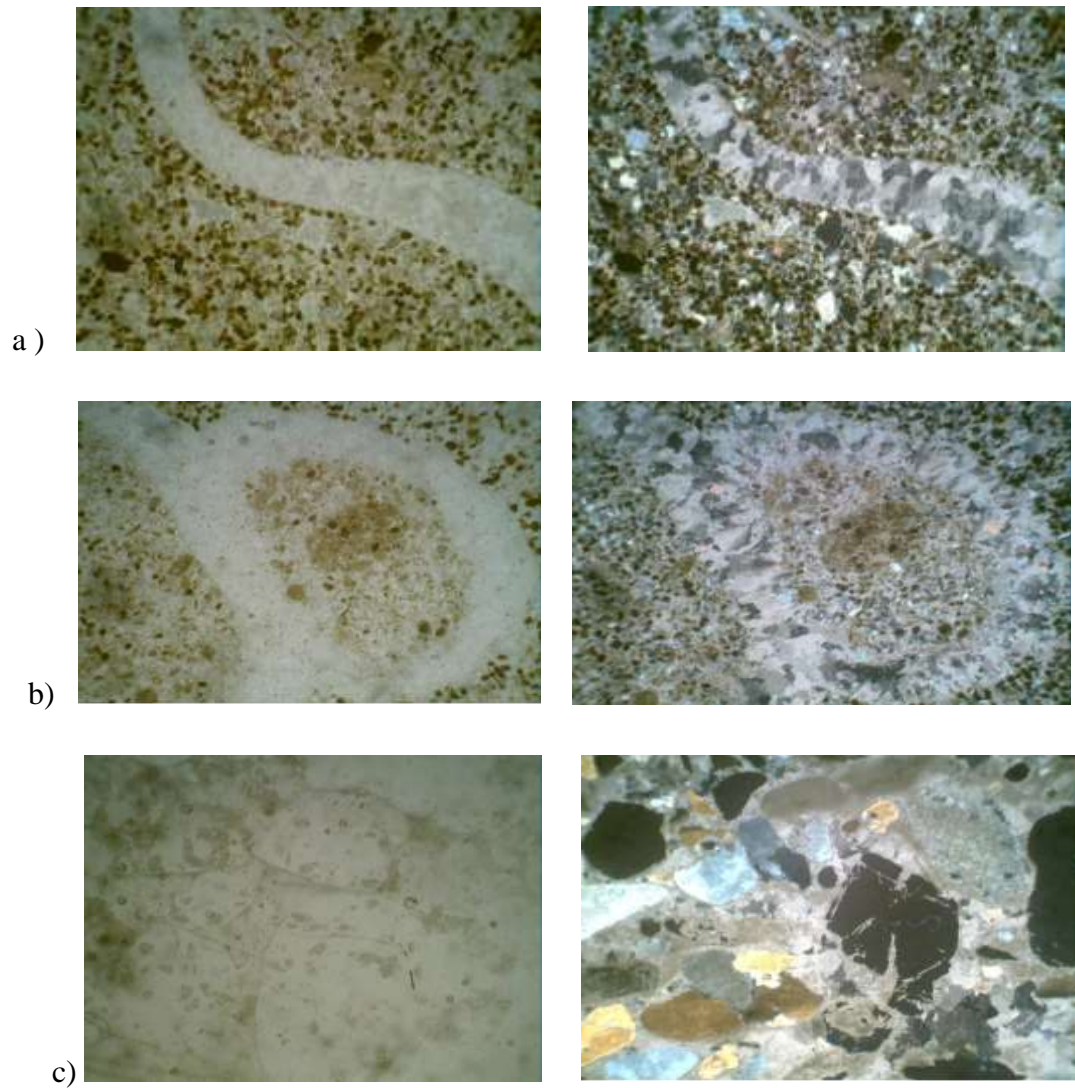


**Fig 6: Photomicrograph of the Itori well limestone a) Bioclast packstone containing sandy quartz grain, few sparite and micrite (IT 13) under PPL and XP b) Sandy Bioclast packstone shows gastropod with infilling sparry calcite cement under PPL and XP c) Bioclast packstone showing intra clast in the fine grain micritic groundmass under PPL and XP (IT17).**



## Geochemistry

### Major oxide geochemistry

The results of major element oxides are shown in Table 4. The elemental oxides for the sandstone have the following ranges; SiO<sub>2</sub> (33.29 - 71.83wt %), Al<sub>2</sub>O<sub>3</sub> (2.03- 3.97wt %), Fe<sub>2</sub>O<sub>3</sub> (1.95-2.40wt %), TiO<sub>2</sub> (0.17 - 0.18wt %) and CaO (11.8 - 31.0wt %). Other oxides such as MgO, Na<sub>2</sub>O, K<sub>2</sub>O, V<sub>2</sub>O<sub>3</sub>, MnO, NiO, ZrO<sub>2</sub>, ZnO, SrO are less than 1 percent (< 1wt %) each. The composition of the limestone are; SiO<sub>2</sub> (13.03 - 53.23wt %), Al<sub>2</sub>O<sub>3</sub> (0.22 - 2.56wt %), Fe<sub>2</sub>O<sub>3</sub> (0.6 - 12.87wt %), TiO<sub>2</sub> (0.02-0.12wt %) and CaO (12.95 - 46.6wt %). Other oxides such as MgO, Na<sub>2</sub>O, K<sub>2</sub>O, V<sub>2</sub>O<sub>3</sub>, MnO, NiO, ZrO<sub>2</sub>, ZnO, SrO are less than 1 percent (< 1wt. %) each. The SiO<sub>2</sub> values for the sandstone indicate low compositional maturity and low to high degree of weathering (Pettijohn, 1963). The concentration of Al<sub>2</sub>O<sub>3</sub> and Fe<sub>2</sub>O<sub>3</sub> in the rock types clear indication of weathering processes (Tijani *et al.*, 2010). The low value of TiO<sub>2</sub> content in the samples suggest more felsic material in the source rocks (Taylor and McLennan, 1985). The high values of CaO in both rock types are associated with the limestone of the Ewekoro Formation in the basin.

### Trace element geochemistry.

The trace element concentrations of the analyzed samples are presented in Table 5. The result show that Ti dominates the trace element suites with value ranging from 373.40 - 944.33ppm (av., 1.048ppm). Others are; P (293.83 - 557.88ppm; av., 576.54ppm); Sr (126.04 - 543.88 ppm; av. 304.54 ppm). The value of Sr is lower than the average values for lithospheric carbonate where Sr= 610 ppm (Turekian and Wedepohl, 1961). Ranges of other trace elements are as follows; Zr (4.65 - 426.17ppm, av 52.05ppm), Cr( 10.82 - 141.73, av 43.0ppm), Zn(15.42 - 268.01, av 79.0ppm), V(5.04 - 258.34ppm, av. 79.0ppm); Th(0.43-11.32ppm,av2.09ppm) and Ba (5.20 - 36.94, av 6.0ppm). The abundance of high field strength elements such as; Cr and Zr, can be related to the presence of detrital minerals such as chrome spinel and zircon (Hunstsman- Mapilaa *et al.*, 2005). Strontium (Sr) and Barium (Ba) are two elements with different geochemical behaviors. According to Liu (1980), the Sr/Ba ratio is regarded as an indicator of paleo- salinity. The trace elements concentrations normalized with the Post – Archean Australian Shale (PAAS) value showed significant variations in transition trace elements (TTE: Sc, Co, Cu, Ni, V, Zn, Cr and Mn) and high field strength elements (HFSE: Zr, Hf and Nb) (Fig. 7 ). Overall, PAAS- normalized

patterns of the samples showed significant enrichment in P, Sr and Cr; whereas Ti, Cs, Th, and U are lower than PAAS (Fig.7).

### **Rare element geochemistry**

The REE concentrations of the analyzed sediments are presented in Table 6. The range of Total  $\Sigma$ REE contents (1.199-226.83 ppm; average = 44.26 ppm; n =12) showed significant variations among the samples. The  $\Sigma$ REE contents are higher than the range for marine carbonates; 0.04-14 ppm (Turekian and Wedepohl, 1961) and average typical marine carbonates ~ 28 ppm (Bellanca *et al.*, 1997). The PAAS- normalized patterns of the samples showed significant enrichment in Gd, Y, Nd, Ce and Sr whereas Lu, Tm, and Tb are lower than PAAS ( Fig.8).

**Table 4: Distribution of major oxide concentration (%) in the study well**

	IT2	IT5	IT13	IT14	IT16	IT17	IT19	IT22	IT26	IT28	IT 30	IT 32	AVG
Oxides	Sandstones		Limestone										
SiO <sub>2</sub>	71.83	33.29	39.18	53.32	51.76	41.35	23.64	43.27	42.65	29.87	22.9	13.03	38.84
Al <sub>2</sub> O <sub>3</sub>	2.03	3.97	2.56	1.47	0.29	0.22	0.95	0.23	0.49	0.33	0.74	0.31	1.13
MgO	0.36	0.64	1.22	1.49	0.62	0.61	1.62	0.87	1.55	0.55	0.54	0.42	0.87
Na <sub>2</sub> O	<0.01	<0.01	<0.01	<0.01	<0.01	<0.01	<0.01	<0.01	<0.01	<0.01	<0.01	<0.01	<0.01
P <sub>2</sub> O <sub>5</sub>	0.18	0.15	0.23	0.34	0.07	0.08	0.25	0.06	0.07	0.06	0.21	0.14	0.15
Fe <sub>2</sub> O <sub>3</sub>	1.95	2.4	7.58	12.87	0.58	0.6	1.56	0.74	0.82	0.64	1.06	0.6	2.62
K <sub>2</sub> O	0.13	0.18	0.16	0.1	0.01	0.01	0.07	0.01	0.02	0.01	0.02	0.01	0.06
CaO	11.48	31	24.31	12.95	24.94	30.16	38.41	29.19	28.3	37.31	40.42	46.6	29.59
TiO <sub>2</sub>	0.18	0.17	0.77	0.26	0.12	0.05	0.06	0.03	0.06	0.02	0.03	0.02	0.15
V <sub>2</sub> O <sub>5</sub>	<0.01	<0.01	0.04	0.01	<0.01	<0.01	<0.01	<0.01	<0.01	<0.01	<0.01	<0.01	0.03
Cr <sub>2</sub> O <sub>3</sub>	0.01	<0.01	0.03	0.01	<0.01	<0.01	<0.01	<0.01	<0.01	<0.01	<0.01	<0.01	0.02
MnO	0.05	0.09	0.08	0.09	0.03	0.03	0.04	0.02	0.02	0.04	0.07	0.05	0.05
NiO	<0.01	<0.01	0.01	<0.01	<0.01	<0.01	<0.01	<0.01	<0.01	<0.01	<0.01	<0.01	0.01
CuO	<0.01	<0.01	<0.01	<0.01	<0.01	<0.01	<0.01	<0.01	<0.01	<0.01	<0.01	<0.01	<0.01
ZrO <sub>2</sub>	0.13	0.07	0.74	0.15	0.1	0.05	0.03	0.05	0.06	0.03	0.02	0.02	0.12
S	0.52	0.53	0.23	0.04	<0.01	<0.01	0.03	0.23	0.06	0.01	0.01	0.01	0.17
C <sub>3</sub> O <sub>4</sub>	<0.01	<0.01	<0.01	0.01	<0.01	<0.01	<0.01	<0.01	<0.01	<0.01	<0.01	<0.01	0.01
ZnO	0.01	0.01	0.04	0.01	<0.01	0.01	<0.01	<0.01	<0.01	<0.01	<0.01	<0.01	0.02
SrO	0.06	0.13	0.07	0.04	0.06	0.08	0.15	0.09	0.1	0.09	0.13	0.12	0.09
WO <sub>3</sub>	<0.01	0.01	0.01	<0.01	<0.01	<0.01	<0.01	<0.01	<0.01	<0.01	<0.01	<0.01	0.01
LOI	11.09	27.35	22.75	16.81	21.4	26.7	33.18	25.15	25.77	31.01	33.82	38.64	26.14

**Table 5: Distribution of trace element concentration (ppm) in the-study well**

ppm	IT2	IT5	IT13	IT14	IT16	IT17C	IT19	IT22	IT26	IT28	IT30	IT32	Total	AVG
	Sandstones		Limestone											
Sc	2.86	5.79	11.81	5.66	0.76	0.70	2.29	0.65	0.95	0.86	2.13	1.29	35.75	2.97
Co	4.83	3.62	9.64	5.17	0.35	0.39	1.91	1.01	0.94	0.71	2.55	1.34	32.46	2.70
Cu	4.13	6.19	5.54	4.18	2.79	3.89	3.17	3.11	3.72	4.49	4.22	5.22	50.64	4.22
Ni	12.10	12.03	20.14	11.50	2.33	2.29	5.38	4.46	4.29	3.73	8.35	4.65	91.25	7.60
V	15.50	21.33	258.34	121.3	5.04	5.23	18.66	5.53	9.08	8.28	22.48	10.70	501.45	41.78
Zn	46.77	49.09	268.01	60.78	19.36	46.99	30.36	15.42	31.40	26.47	52.60	21.31	668.55	55.8
Cr	23.87	31.82	141.73	52.48	14.52	13.47	25.73	10.82	33.97	17.12	32.52	27.17	425.21	43.0
Zr	27.51	22.09	426.17	86.22	9.76	9.18	11.26	4.65	9.29	6.17	7.67	4.70	624.67	52.05
Cs	0.34	0.70	0.31	0.21	0.07	0.07	0.23	0.08	0.15	0.10	0.18	0.10	2.53	21.0
Hf	0.84	0.55	10.64	2.45	0.28	0.24	0.32	0.13	0.24	0.17	0.22	0.13	16.20	35.0
Nb	2.17	3.22	7.31	3.11	1.07	1.54	1.12	0.62	1.08	0.58	0.79	0.64	23.24	94.0
Rb	5.26	10.36	6.26	3.62	1.33	1.31	4.61	1.76	3.03	2.23	3.21	1.74	44.73	73.0
Sr	141.9	389.38	213.78	126.4	155.63	257.88	543.14	282.95	304.31	330.50	449.03	460.24	3654.83	304.6
Th	1.60	1.92	11.32	3.71	0.59	0.43	1.06	0.49	0.92	0.65	1.57	0.88	25.12	2.09
U	1.06	1.17	2.46	0.87	0.36	0.35	1.96	0.63	0.49	0.32	0.98	0.45	11.11	0.93
Ba	24.95	27.92	36.94	36.91	6.42	5.20	12.14	6.04	8.15	9.50	10.77	7.11	192.03	16.00
Pb	4.76	4.04	17.74	7.39	2.30	1.30	1.62	2.07	2.44	1.59	4.43	2.51	52.19	4.35
P	549.9	550.88	551.88	552.9	553.88	554.88	555.88	556.88	557.88	293.83	977.39	662.32	6918.48	576.5
Li	22.17	53.33	19.18	10.02	3.54	3.01	10.42	2.90	5.74	2.98	6.28	2.89	142.45	11.87
Sb	0.36	0.14	0.43	0.32	0.09	0.08	0.07	0.19	0.14	0.11	0.21	0.10	2.25	0.19
Ta	0.15	0.19	0.46	0.23	0.06	0.23	0.07	0.03	0.06	0.04	0.05	0.05	1.61	0.13
W	0.48	0.30	0.67	0.31	0.43	1.05	0.13	0.11	0.19	0.47	0.70	0.90	5.73	0.48
Tl	0.03	0.03	0.02	0.01	-0.00	-0.00	0.00	0.00	-	0.00	0.01	0.00	0.10	0.01
AS	5.14	0.94	3.20	1.84	0.14	0.15	0.50	0.62	0.42	1.60	1.07	0.55	16.16	1.35
Ga	3.23	5.26	5.92	3.26	0.85	0.65	2.60	0.82	1.52	1.12	3.00	1.55	29.78	2.48
Ti	944.3	127.34	436.14	1427	849.02	373.40	777.41	495.30	697.04	448.06	457.89	476.25	11307	1027
P/Ti	0.58	0.43	0.013	0.39	0.66	1.49	0.715	1.12	0.8	0.66	2.14	1.39	10.39	0.87
U/Th	0.66	0.61	0.22	0.24	0.61	0.81	1.85	1.29	0.53	0.49	0.62	0.51	8.44	0.70
V/Cr	0.65	0.67	1.822	2.31	0.35	0.39	0.73	0.51	0.27	0.48	0.69	0.37	9.24	0.77
Ni/co	2.51	3.31	2.04	2.23	6.66	5.87	2.81	4.41	4.56	5.25	3.27	3.47	46.39	3.87
Sr/Ba	5.69	13.95	5.79	3.41	24.24	49.59	44.74	46.85	37.34	34.79	41.69	64.73	372.81	31.07
Cu/Zn	0.09	0.13	0.02	0.07	0.14	0.08	0.07	0.20	0.12	0.17	0.08	0.24	1.41	0.12
Zr/Rb	5.23	0.21	68.08	23.81	7.33	7.43	2.44	2.64	3.07	2.77	2.39	2.70	128.10	10.68

Th/Cr	0.07	0.06	0.08	0.07	0.04	0.03	0.06	0.05	0.03	0.04	0.05	0.03	0.61	0.05
Cr/Th	14.29	16.67	12.50	14.29	25.00	33.30	16.67	20.00	33.30	25.00	20.00	33.30	264.32	22.03
Th/Sr	0.56	0.33	0.96	0.66	0.78	0.61	0.46	0.75	0.97	0.76	0.73	0.68	8.25	0.69
Th/Co	0.33	0.53	1.17	0.71	0.89	1.10	0.55	0.49	0.98	0.92	0.62	0.66	8.95	0.75
V/(V/ Ni)	0.56	0.64	0.93	0.91	0.68	0.70	0.78	0.55	0.68	0.70	0.73	0.70	8.56	0.71
Sr/Cu	34.37	62.90	38.59	30.15	55.78	66.29	171.34	90.98	97.85	73.61	106.41	88.17	916.44	76.37
Th/Sc	0.56	0.33	0.96	0.66	0.78	0.61	0.46	0.75	0.97	0.76	0.74	0.68	8.22	0.69
Th/U	1.51	1.64	4.60	4.26	1.64	1.23	0.54	0.78	1.88	2.03	1.60	1.96	23.67	1.97
Rb/Sr	0.04	0.03	0.03	0.03	0.009	0.005	0.08	0.06	0.01	0.007	0.007	0.004	0.31	0.03
Zr/Rb	5.23	2.13	68.30	23.82	7.34	6.9	2.44	2.64	2.82	2.77	2.39	2.70	129.48	10.79

**Table 6: Distribution of rare element concentration (ppm) for the study well**

Ppm	IT2	IT5	IT13	IT14	IT16	IT17C	IT19	IT22	IT26	IT28	IT30	IT32	ΣREE	AVG
	Sandstones		Limestone											
La	10.325	15.26	19.52	12.604	4.06	3.107	10.472	4.303	6.837	5.807	18.162	8.029	118.486	9.87
Ce	20.093	27.198	48.302	31.116	6.351	4.829	21.936	6.591	11.188	8.289	28.409	12.54	226.839	8.90
Pr	2.218	2.95	4.979	3.242	0.88	0.695	2.486	0.948	1.625	1.34	3.984	1.827	27.174	2.26
Nd	8.812	11.182	20	13.013	3.67	2.856	10.397	3.976	6.808	5.603	16.264	7.669	110.25	9.19
Sm	1.669	1.891	4.344	2.57	0.715	0.595	1.915	0.807	1.285	1.095	3.087	1.497	21.47	1.79
Eu	0.378	0.42	1.053	0.619	0.171	0.143	0.445	0.192	0.297	0.256	0.704	0.342	5.02	0.42
Gd	1.522	1.575	4.116	2.315	0.694	0.596	1.726	0.779	1.163	1.028	2.727	1.37	19.611	1.63
Tb	0.205	0.207	0.629	0.326	0.098	0.083	0.224	0.109	0.153	0.141	0.375	0.185	2.735	0.23
Dy	1.168	1.19	3.783	1.903	0.577	0.505	1.25	0.639	0.875	0.825	2.143	1.053	15.911	1.33
Y	6.151	6.939	20.267	9.11	3.58	3.486	7.985	4.436	5.55	5.802	13.751	7.708	94.765	7.90
Ho	0.224	0.228	0.747	0.36	0.115	0.099	0.228	0.127	0.169	0.16	0.403	0.212	3.072	0.26
Er	0.615	0.615	2.154	0.977	0.312	0.268	0.586	0.341	0.446	0.427	1.058	0.547	8.346	0.70
Tm	0.089	0.088	0.342	0.149	0.045	0.038	0.078	0.047	0.059	0.059	0.145	0.075	1.214	0.10
Yb	0.57	0.566	2.373	0.96	0.281	0.232	0.49	0.281	0.366	0.344	0.86	0.454	7.777	0.65
Lu	0.086	0.087	0.377	0.145	0.043	0.035	0.074	0.043	0.055	0.052	0.131	0.071	1.199	0.10

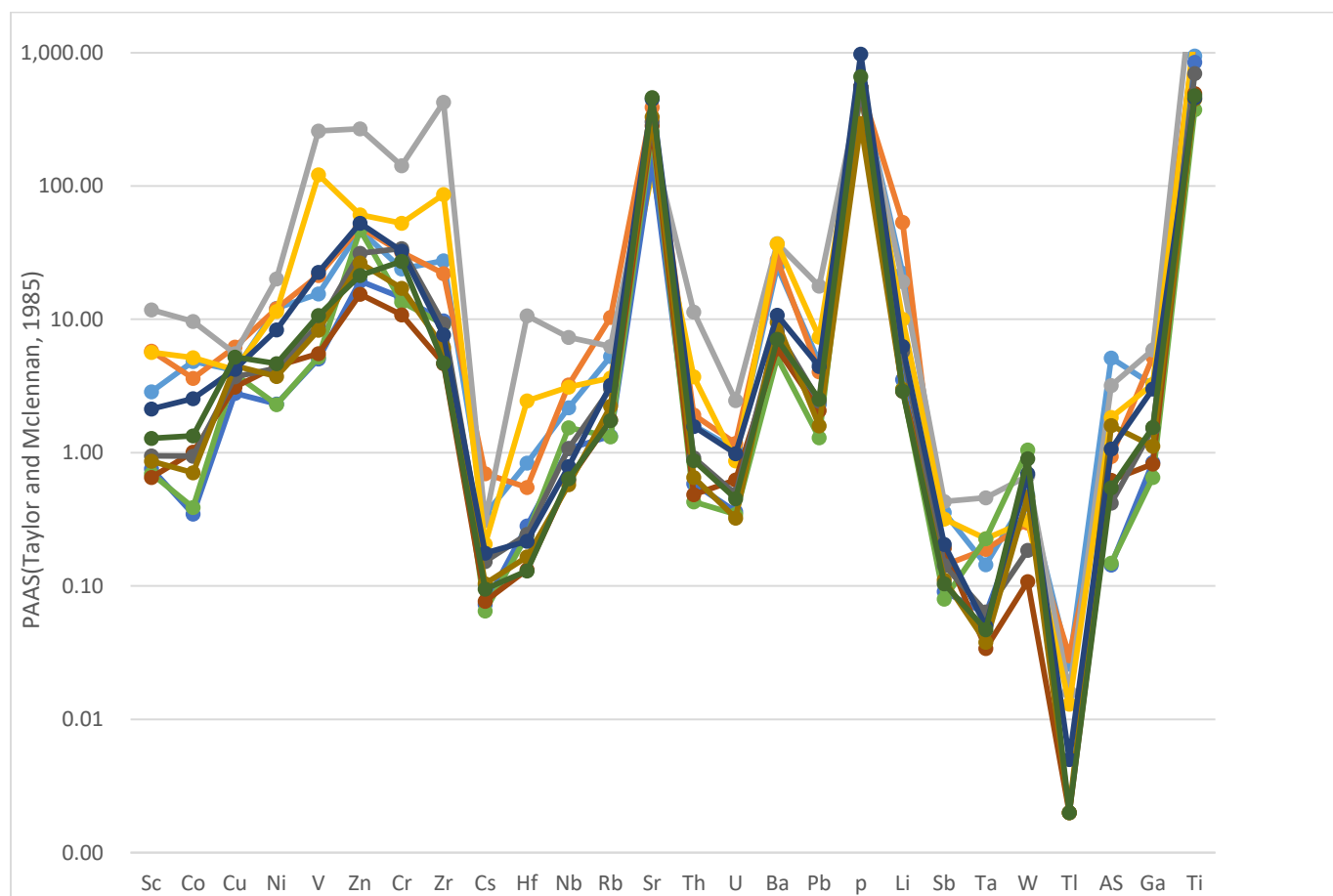


Fig 7: PASS- normalized trace element distribution of Itori well.

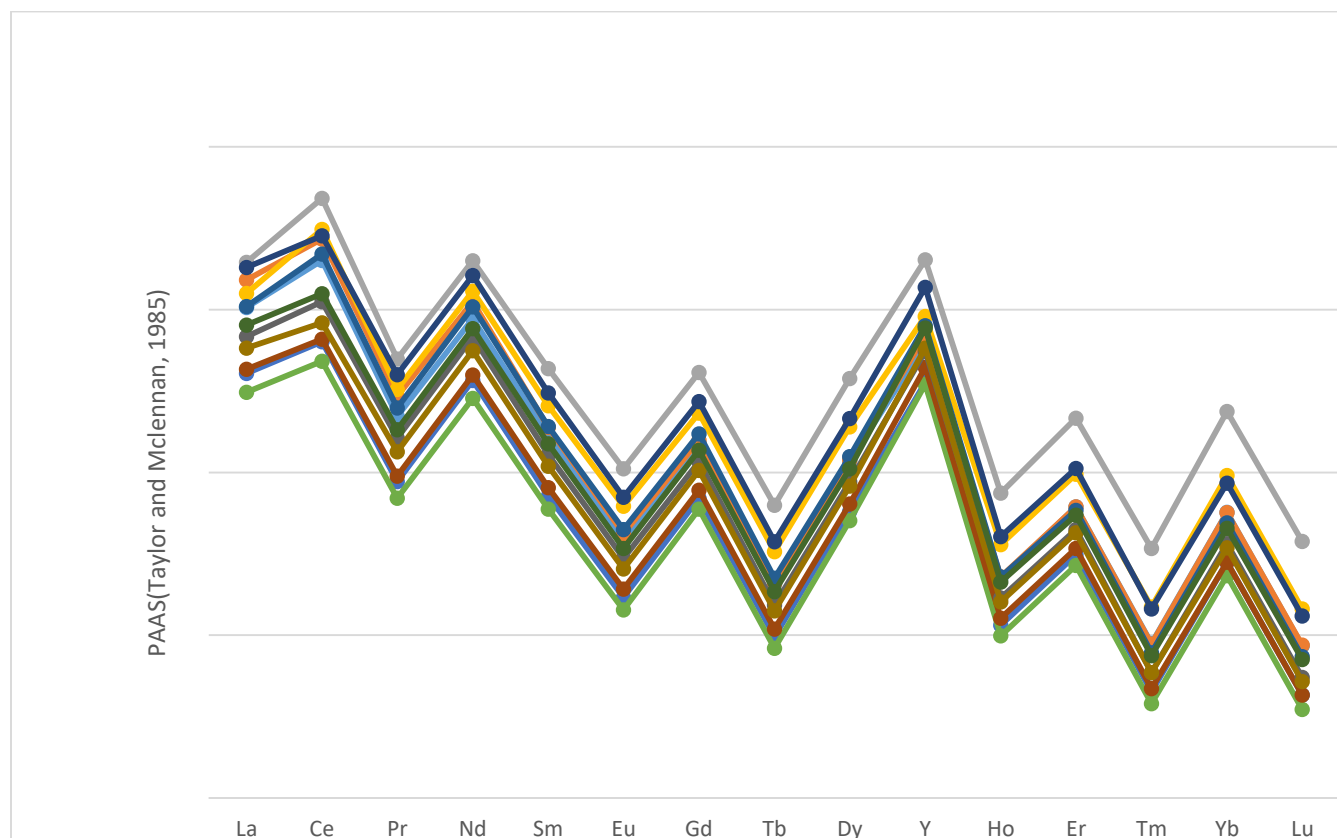


Fig 8: PAAS- normalized rare element distribution of Itori well.



## **Provenance**

Some elemental ratios such as; Th/Sc, Th/Co and Th/Cr, Cr/Th, show significant variations in felsic and mafic rocks and are widely used to investigate the source area composition (Wronkiewicz and Condie, 1990; Cox *et al.*, 1995; Cullers, 1995; Armstrong-Altrin *et al.*, 2004; Armstrong-Altrin, 2009). The Th/Sc, Th/Co and Th/Cr, Cr/Th ratios of the study well, compared with those of sediments derived from felsic and mafic rocks as well as to average values of upper continental crust (UCC) and PAAS values (Table 7) suggest intermediate to felsic provenance for the sediments (Table 7). Modal sandstone composition consists of sub rounded quartz grain, monocrystalline and polycrystalline quartz grains, rock fragment, rutile, garnet and tourmaline, suggest a mixed provenance of metamorphic, plutonic and recycled sedimentary sources of southwestern Nigeria.

## **Tectonic Setting**

Several authors such as; (Maynard *et al.*, 1982; Bhatia, 1983; Bhatia and Crook 1986; Roser and Korsch, 1986; Kroonenberg 1994) have related sandstone geochemistry to specific tectonic environment. Inert trace elements in clastic sediments have also been used successfully in discrimination diagrams of plate tectonic settings (Varga and Szakmany, 2004; Elzien *et al.*, 2014), these elements are probably transferred quantitatively into detrital sediments during weathering and transportation, reflecting the signature of the parent material (Armstrong-Altrin *et al.*, 2004). From the cross plot of  $K_2O/Na_2O$  vs  $SiO_2$ , (Roser and Korsch, 1986) (Fig 9), it was established that the sediments plotted dominantly in the Active Continental Margin and Passive Continental Margin, suggesting a syn-rift faulting setting of a transform margin. It also suggested that the sediments comes from multiple sources, of igneous and metamorphic basement rocks plus reworked older clastic sediments (fig 10a and b) (Madukwe *et al.*, 2015). Cross plot of  $SiO_2$  against total  $Al_2O_3 + K_2 + Na_2O$  (Fig11) also shows a semi humid climatic condition with increase chemical maturity.

### **Paleo-redox conditions.**

Redox sensitive elements, e.g. V, U, Fe, Mn, Co, Cr, and Ni, indicate the redox characteristics of the depositional environment as they are immobile after deposition and burial (Jones and Manning, 1994). That is why redox sensitive elements are ideal and reliable proxies for interpreting paleo-redox conditions of sedimentary rocks (Goldberg and Humayun, 2016;). In this study, the paleo-redox conditions were defined using reference standards for U/Th, V/Cr, Ni/Co, and V/(V + Ni). Commonly, V/Cr ratios > 4.25 signify an anoxic depositional environment, i.e., exhibit strong reducing conditions. Ratios between 2.0 and 4.25, indicate a dysoxic depositional setting, i.e. reducing conditions. Ratios <2.0 point to an oxic depositional environment, i.e. oxidizing conditions (Li *et al.*, 2018). Similarly, Ni/Co values >7.0 show an anoxic depositional environment, 5.0–7.0 indicates a dysoxic environment, and <5.0 suggests oxic conditions (Jones and Manning, 1994; Guo *et al.*, 2011). U/Th ratios >1.25 indicate anoxic conditions, 0.75–1.25 reflect dysoxic conditions, and <0.75 show oxic conditions (Jones and Manning, 1994). Finally, V/ (V + Ni) ratios >0.84 indicate euxinic depositional conditions, i.e. anaerobic-reducing conditions, 0.54–0.82 indicates anoxic settings, and 0.46–0.60 indicates dysoxic depositional conditions (Hatch and Leventhal, 1992). From the studied well, V/Cr ranges from 0.27-2.31(av. 0.77ppm) indicating sediment deposition under oxic condition. The values of Ni/Co range from 2.04-5.87ppm (av. 3.87) also suggesting an oxic condition. U/Th value ranges from 0.22 -0.62ppm (avg 0.77pm) indicating deposition of sediment in dysoxic condition. In addition, V/(V + Ni ) ratio ranges 0.55- 0.93ppm ( av. 0.71ppm) Table 5, indicating deposition in an anoxic. It can be concluded that Itori well sediments were deposited in a strongly oxic through dysoxic to anoxic condition (Nton and Adeyemi, 2014). In addition, high Cu/Zn ratios in a sedimentary environment reflect reducing depositional conditions, whereas low Cu/Zn values indicate oxidizing depositional conditions (Hallberg, 1976). The Cu/Zn in the studied well ranges from 0.02- 0.24 indicating an oxidizing environment.

### **Paleo-productivity**

Geochemical indicators, such as the abundance of selected elements (Ba, P, Cu, Ni, and Zn) have been used to indicate the changes in primary productivity (Schenau *et al.*, 2005; Schoepfer *et al.*, 2015). Paleo-productivity indicates the quantity of organic matter that organisms can generate per unit area and time during the energy cycle (Chen *et al.*, 2021a). The trace element ratios of P/Ti

provide valuable information on nutritional conditions and paleo-productivity, i.e. the uptake of dissolved inorganic carbon and its sequestration into organic compounds by primary marine producers (Tribovillard *et al.*, 2006; Li *et al.*, 2020; Zhang *et al.*, 2020). Phosphorus is important for all kinds of life on earth since it is a major component of skeletal material and is involved in a variety of metabolic activities (Li *et al.*, 2020; Zhang *et al.*, 2021). Li *et al.*, (2020) provided the following thresholds; P/Ti value < 0.34 lower; 0.34–0.79 intermediate, and P/Ti >0.79 indicates high productivity (Li *et al.*, 2020). In this study, the P/Ti ratio ranges from 0.013-2.14ppm (average 0.87ppm) Table 5, indicating high productivity.

### **Paleo-hydrodynamic conditions**

This describes the energy condition of the water mass during the deposition of ancient sedimentary rocks (Pehlivanli, 2019). According to Pehlivanli, (2019), Zr is a common continental inert element that is preserved in continental, transitional and shallow-marine environments Rb is a common mobile element in a variety of different geological processes, and it is accumulated in deep water with low energy due to its active chemical properties (Li *et al.*, 2018b). The Zr/Rb ratio can react to changes in water depth and therefore is considered a good indicator for paleo-hydrodynamic condition (Teng, 2004; Teng *et al.*, 2005; Zhao *et al.*, 2016; Li *et al.*, 2018b; Pehlivanli, 2019). The lower the Zr/Rb ratio, the greater the water depth and the weaker the hydrodynamic pressure (Li *et al.*, 2018b; Pehlivanli, 2019). A higher Zr/Rb ratio indicates shallow water circulation and stronger hydrodynamic pressure. In this study, the Zr/Rb ratio ranged from 0.21 - 68.08 (av., 10.97 ppm) Table 5, indicating deposition of sediments under intermediate to strong paleo-hydrodynamic condition (Teng, 2004; Pehlivanli, 2019).

**Table 7: Range of elemental ratios in this study compared to the ratios in sediments derived from felsic rocks, mafic rocks, Upper Continental Crust (UCC) and Post-Archean Australian shale (PAAS).**

Elemental ratio	Range for present study <sup>1</sup>		Range of sediment <sup>2</sup>		UCC <sup>3</sup>	PAAS <sup>3</sup>	Remark on provenance
	Min	Max	Felsic rock	Maficrock			
Th/Sc	0.3	0.97	04.0-0.94	0.71-0.95	0.63	0.66	Intermediate-felsic rock
Th/Co	0.33	0.89	0.67-19.40	0.04-1.40	0.63	0.63	Intermediate-felsic rock
Th/Cr	0.03	0.08	0.13-2.70	0.02-0.05	0.13	0.13	Intermediate-felsic rock
Cr/Th	12.50	33.30	4.00-15.00	25-500	7.76	7.53	Intermediate-felsic rock

<sup>1</sup>Present study, n = 12, <sup>2</sup>(Cullers 1994, 2000; Cullers and Podkovyrov, 2000; Cullers et al. (1988); <sup>3</sup>Taylor and McLennan, 1985)

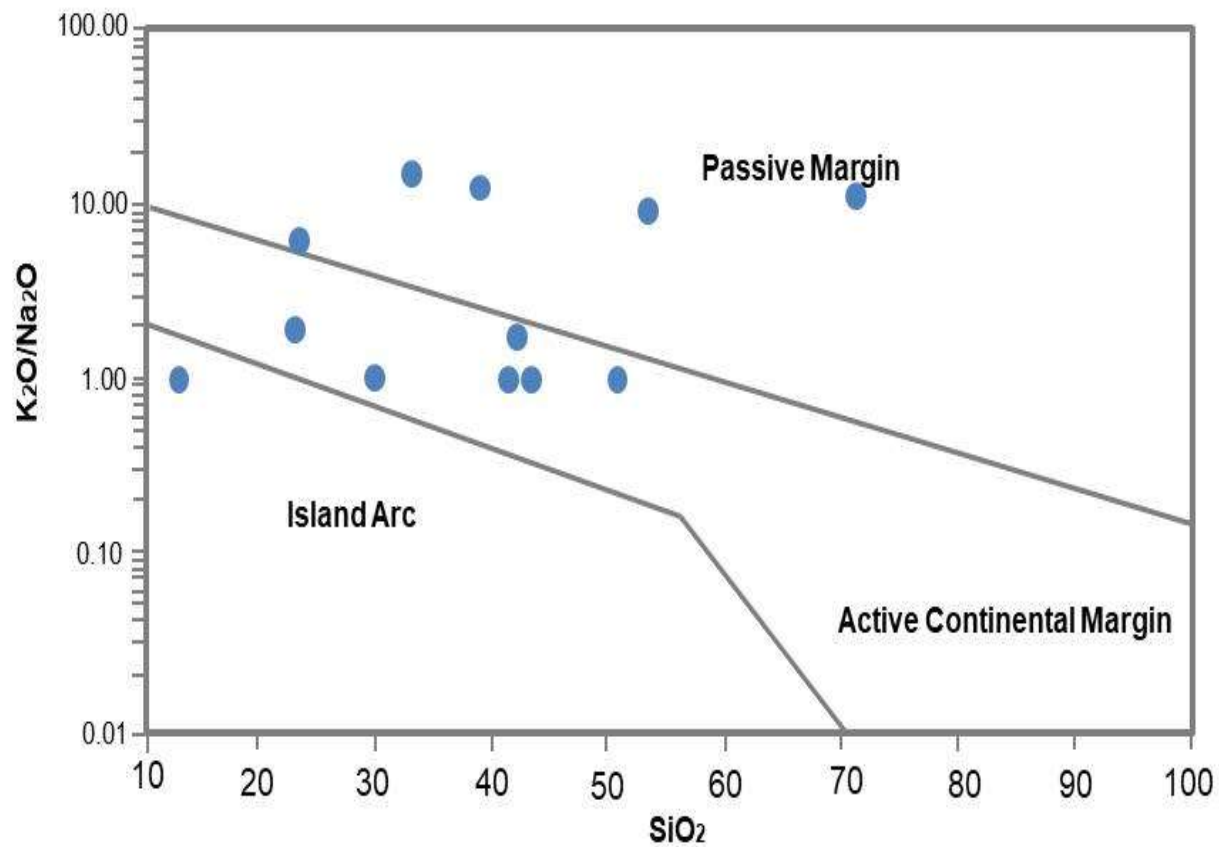


**Fig 9: Provenance discrimination diagram of Roster and Korsch (1986) for Itori well sandstone**

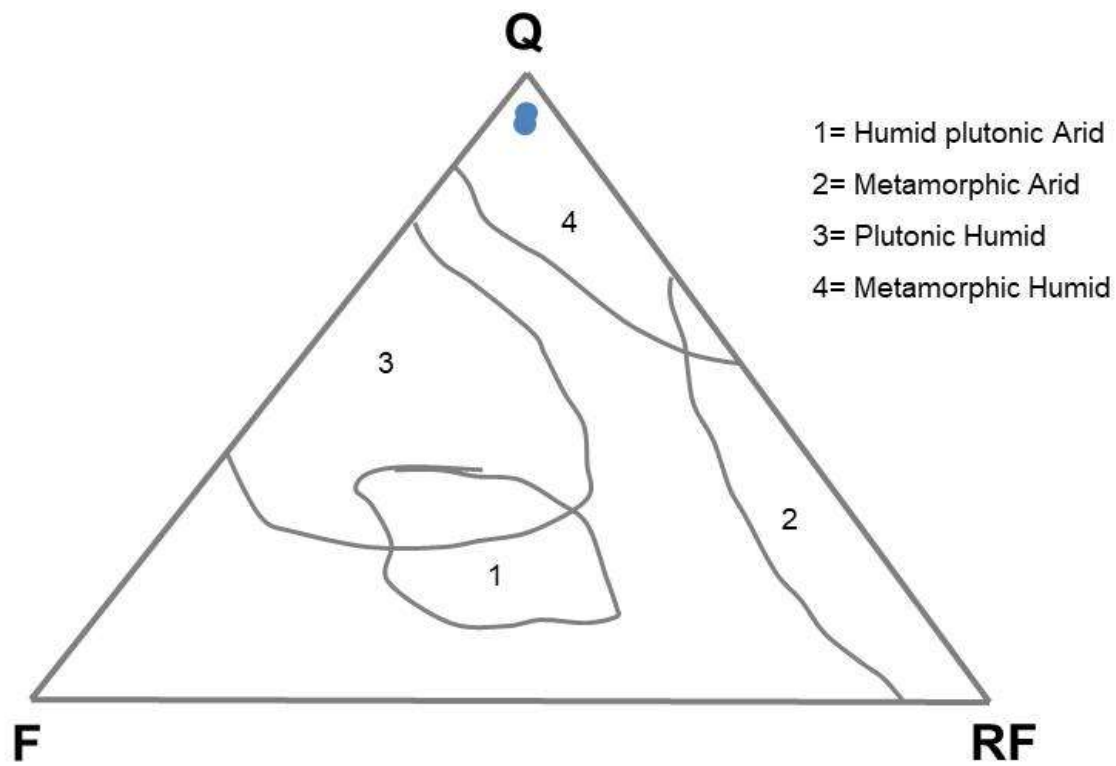


**Fig 10 a. Ternary plot of QFR showing the paleoclimatic setting of Itori well sandstone samples (After: Suttner *et al* 1981)**

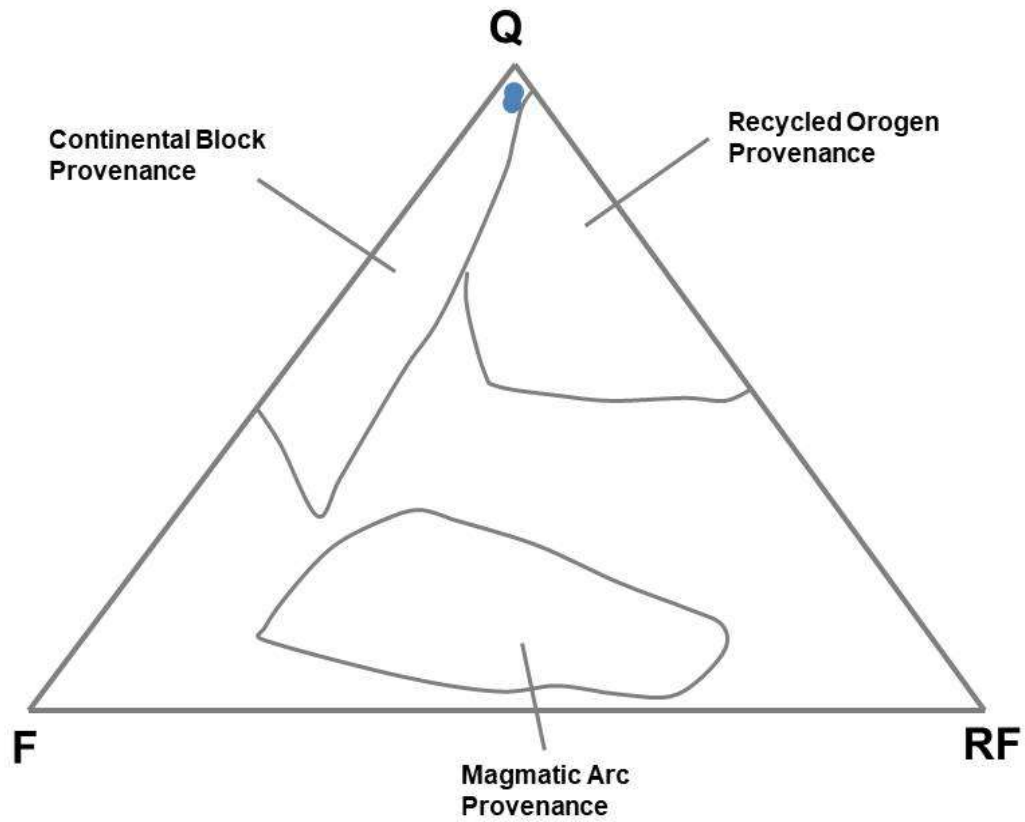


**Fig 10 b Ternary plot of QFR showing paleo- tectonic settings of Itori well sandstone samples (After: Dickinson and Suczek, 1979).**

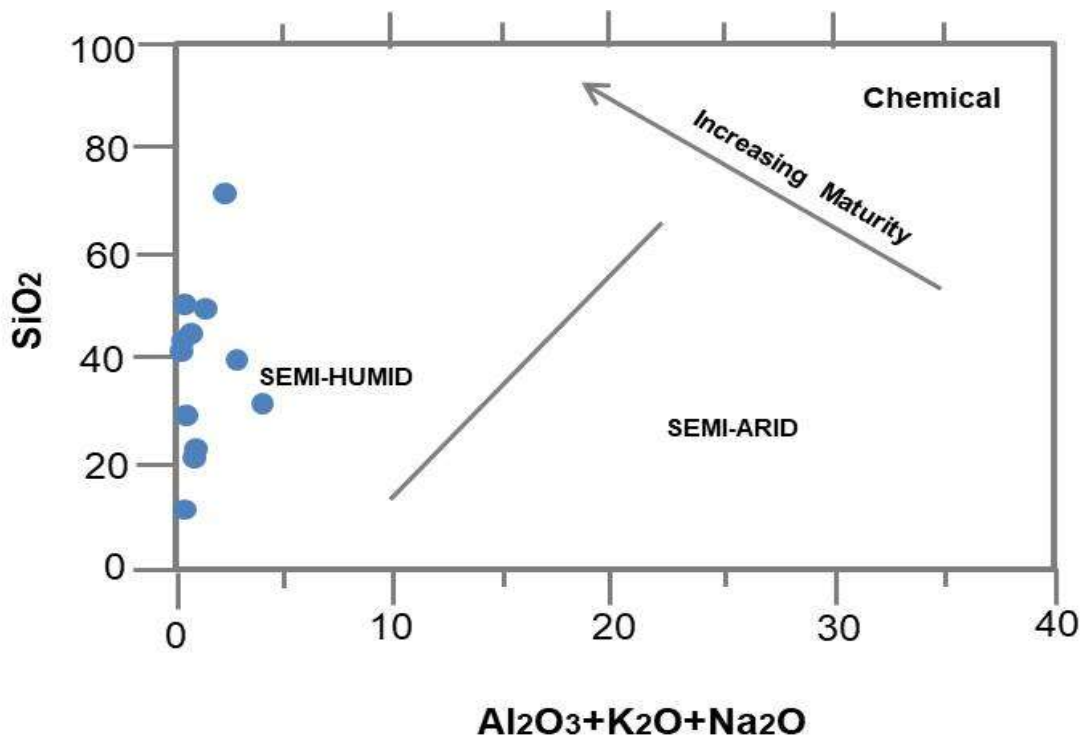


**Fig 11:  $\text{SiO}_2$  against total ( $\text{Al}_2\text{O}_3 + \text{K}_2 + \text{Na}_2\text{O}$ ) showing trend of maturity and paleoclimatic conditions (After: Suttner and Dutta, 1986).**



## **Conclusion and Recommendation.**

Sedimentological and compositional studies were carried out on subsurface samples of Itori well, within the eastern Dahomey Basin. The study aimed at determining the lithofacies association, provenance, tectonic setting, paleo- depositional environment, paleo-climatic, paleo-weathering condition, paleo- productivity and paleo-salinity of the sediments. The sandstone samples classified as Quartz Arenite. The limestone on the other hand revealed two microfacies namely; Sandy Bioclast packstone bioclastic – wackstone-packstone. The Th/Sc, Th/Co and Th/Cr, Cr/Th ratios of the sediments suggest intermediate to felsic provenance for the sediments. Ternary plot of the sandstone revealed metamorphic humid climate setting. Cross plot of  $K_2O/Na_2O$  vs  $SiO_2$ , revealed Active Continental Margin and Passive Continental Margin tectonic setting. Also, a bivariate plot of  $SiO_2$  against total  $(Al_2O_3 + K_2O + Na_2O)$  revealed the prevalence of semi- humid conditions for the sediments with increasing chemical maturity. The ratio of V/Cr ranged from 0.27-2.31(av. 0.77ppm) indicating deposition under oxic condition V/Cr ranged from 0.27-2.31(av. 0.77ppm) indicating deposition under oxic condition

## REFERENCES

- Adediran, S.A and Adegoke, O.S., (1991).** The continental sediment of the Nigerian coastal basins. *Journal of Africa Earth science*. 12(1/2), 79-84.
- Adegoke ,O.S., Ako, B.D., and Enu, E.I. (1980).** Geotechnical investigations of the Ondo State bituminous sands. Vol. 1. Geology and reserve estimate. Rept. Geological Consulting Unit, Dept. of Geology, University of Ife. 257pp
- Adegoke, O.S. (1969);** Eocene Stratigraphy of Southern Nigeria. *Bulletining Bureau de Research Geologic ET Miners Memoir*, 69, 23-48.
- Agagu, O.A. (1985):** A Geological Guide to Bituminous Sediments in South Western Nigeria. Unpublished Report, Department of Geology, University of Ibadan, Ibadan.
- Akaegbobi and Ogungbesan (2016):** Geochemistry of the Paleocene Limestones of Ewekoro Formation. *Ife Journal of Science* vol. 18, no. 3.
- Akpo, B.D (1980):** Stratigraphy of Oshosun Formation in Southwestern Nigeria. *Journal of Mining and Geology* Vol .1(1):77-106.
- Algeo, T.J., and Tribovillard, N. (2009):** Environmental analysis of paleoceanographic systems based on molybdenum-uranium covariation. *Chem. Geol.* 268, 211–225.
- Armstrong-Altrin, J.S., Lee, Y.I., Verma, S.P., and Ramasamy, S. (2004):** Geochemistry of sandstones from the Upper Miocene Kudankulam Formation Southern India: implications for provenance, weathering and tectonic setting. *J. Sediment. Res.* 74, 285–297.
- Armstrong-Altrin, J.S., Verma, S.P., Madhavaraju, J., Lee, Y.I., and Ramasamy, S. (2003):** Geochemistry of Late Miocene Kudankulam Limestones, South India *International Geology Review*, 45, 16–26.
- Bhatia, M.R. (1983). Plate tectonics and geochemical composition of sandstones: *Journal of Geology*. 91, 611-627
- Bechtel, A., Jia, J.L., Strobl, S.A.I., Sachsenhofer, R.F., Liu, Z., Gratzner, R. and Püttmann, W., (2012):** Paleoenvironmental conditions during deposition of the Upper Cretaceous oil shale sequences in the Songliao Basin (NE China): implications from geochemical analyses. *Org. Geochem.* 46, 76–95.
- Bellanca, A., Claps, M., Erba, E., Masetti, D., Neri, R., Premoli-Silva, I., and Venezia, (1996),** Orbitally induced limestone/marlstone rhythms in the Albian-Cenomanian Cismon section (Venetian region, northern Italy): Sedimentology, calcareous and siliceous plankton distribution, elemental and isotope geochemistry. *Palaeogeography, Palaeoclimatology, Palaeoecology*, v. 126, p.14 227–260.
- Berggren, W. A., (1960).** Paleocene Biostratigraphy and Planktonic Foraminifera of Nigeria (West Africa), *Proc. 21st Inter. Geol. Cong. Copenhagen*, 6, 41-55.
- Billman, H.G., (1992):** Offshore Stratigraphy and Paleontology of the Dahomey Embayment, West Africa. *Nigerian Association Petroleum Explorationists Bulletin*, 7, 121-130.

**Brownfield, M.E. and Charpentier, R.R., (2006):** Geology and Total Petroleum Systems of the Gulf of Guinea Province of West Africa: U.S Geological Survey Bulletin 2207-C, 32p.

**Chen, L., Jiang, S., Chen, P., Chen, X., Zhang, B., Zhang, G., Lin, W., Lu, Y., (2021).**Relative sea-level changes and organic matter enrichment in the Upper Ordovician-Lower Silurian Wufeng-Longmaxi Formations in the Central Yangtze area, China.Mar. Pet. Geol. 124, 104809.

**Chen, Q., Li, Z., Dong, S., Yu, Q., Zhang, C., Yu, X., (2021):** Applicability of chemical weathering indices of eolian sands from the deserts in northern China. CATENA 198,105032.

**Cheng, Y., Liu, W., Wu, W., Zhang, Y., Tang, G., Liu, C., Nie, Q., Wen, Y., Lu, P. and Zhang, C., (2021):** Geochemical characteristics of the lower Cambrian Qiongzhusi Formation in Huize area, east Yunnan: implications for paleo-ocean environment and the origin of black rock series. Arab. J. Geosci. 14, 1–16.

**Chivas, A.R., Deckker, P. and Shelley, J.M.G., (1986):** Strontium content of Ostracoda indicates paleosalinity. Nature 316, 251–253.

**Cox, R., Low, D.R., and Cullers, R.L. (1995):** The influence of sediment recycling and basement composition on evolution of mudrock chemistry in the southwestern United States. Geochimica et Cosmochimica Acta, 59, 2919–2940.

**Culler R.L., (2000):** The geochemical of shales, siltstone and Sandstone vof Pennsylvania-Permian age, Colorado, USA: Implications for provenance and metamorphic studies. Chemical Geology. 51,181-203.

**Cullers, R.L. (1994):**The controls on the major and trace element variation of shales, siltstones and sandstones of Pennsylvanian – Permian age from uplifted continental blocks in Colorado to platform sediment in Kansas, USA: Geochimica et Cosmochimica Acta, 58(22), 4955-4972.

**Cullers, R.L. (1995):** The controls on the major and trace element evolution of shales, siltstones and sandstones of Ordovician to Tertiary age in the Wet Mountain region, Colorado, U.S.A. Chemical Geology, 123, 107–131.

**Cullers, R.L. (2000):** The geochemistry of shales, siltstones and sandstones of Pennsylvanian-Permian age, Colorado, U.S.A.: implications for provenance and metamorphic studies: Lithos, 51, 305-327.

**Cullers, R.L. and Podkovyrov, V.N. (2000):** Geochemistry of the Mesoproterozoic Lakhanda shales in southeastern Yakutia,Russia: implications for mineralogical and provenance control, and recycling. NO JOURNAL

**Cullers, R.L., Basu, A. and Suttner, L. (1988):** Geochemical signature of provenance in sand-size material in soils and stream sediments near the Tobacco Root batholith, Montana, USA: Chemical Geology, 70(4), 335- 348.

**Deng, H.W., Qian, K., (1993):** Sedimentary Geochemistry and Environment Analysis. GansuTechnology Publishing House, Lanzhou, pp. 1–150.

Dickinson, W. R. (1970). Interpreting detrital model of greywacke and arkose. Journal of Sedimentary Petrology, 40, 695 – 707

**Elueze, A. A. and Nton, M. E. (2004):** Organic geochemical appraisal of limestones and shales in part of eastern Dahomey Basin, southwestern Nigeria. *Journal of Mining and Geology*, Vol.40 No.1, 29-40

**Fayose, E. A. and Asseez, L. O., (1972):** Micropaleontological investigation of Ewekoro area, southwestern Nigeria. *Micropaleontology*, 18, (3), 369 – 385.

**Fayose, E.A. (1970):** Stratigraphic paleontology of Afowo-1 well, SW Nigeria. *J. Min. Geol. Nig.* 5(1), 23-34.

**Fayose, E.A. and Azeez, L.O. (1972);** Micropalaeontological Investigations of Ewekoro Area, Southwestern Nigeria. *Micropaleontology*, 18, 369-385.<http://dx.doi.org/10.2307/1485014>.

**Fedo, C.M., Wayne Nesbitt, H., and Young, G.M., (1995):** Unraveling the effects of potassium metasomatism in sedimentary rocks and paleosols, with implications for paleoweathering conditions and provenance. *Geology* 23, 921–924.

**Goldberg, K. and Humayun, M., (2016):** Geochemical paleoredox indicators in organic-rich shales of the Irati Formation, Permian of the Parana Basin, southern Brazil. *Brazilian J. Geol.* 46, 377–393.

**Goldberg, K., and Humayun, M., (2016):** Geochemical paleoredox indicators in organic-rich shales of the Irati Formation, Permian of the Parana Basin, southern Brazil. *Brazilian J. Geol.* 46, 377–393.

**Hallberg, R.O., (1976):** A geochemical method for investigation of palaeoredox conditions in sediments. *Ambio Special Rep.* 4, 139–147.

**Hatch, J.R., and Leventhal, J.S., (1992):** Relationship between inferred redox potential of the depositional environment and geochemistry of the Upper Pennsylvanian (Missourian) Stark Shale Member of the Dennis Limestone, Wabaunsee County, Kansas, USA. *Chem. Geol.* 99, 65–82.

**Huang, H., He, D., Li, D., Li, Y., Zhang, W., Chen, J., (2020).** Geochemical characteristics of organic-rich shale, Upper Yangtze Basin: implications for the Late Ordovician–Early Silurian orogeny in South China. *Palaeogeogr. Palaeoclimatol. Palaeoecol.* 554, 109822.

**Jones, B. and Manning, D.A.C., (1994):** Comparison of geochemical indices used for the interpretation of palaeoredox conditions in ancient mudstones. *Chem. Geol.* 111, 111–129.

**Jones, H.A. and Hockey, R.D. (1964):** The Geology of Part of Southwestern Nigeria. *Geological Survey of Nigeria Bulletin*, 31, 1-101.

**Kahmann, J.A., Seaman, J. and Driese, S.G., (2008):** Evaluating trace elements as paleoclimate indicators: multivariate statistical analysis of late Mississippian Pennington Formation paleosols, Kentucky, USA. *J. Geol.* 116, 254–268.

**Li, D., Li, R., Zhu, Z., Wu, X., Liu, F., Zhao, B., Cheng, J., Wang, B., (2018).** : Elemental characteristics and paleoenvironment reconstruction: a case study of the Triassic lacustrine Zhangjiatan oil shale, southern Ordos Basin, China. *Acta Geochim.* 37, 134–150.

- Li, D., Li, R., Zhu, Z., Xu, F., (2018):** Elemental characteristics of lacustrine oil shale and its controlling factors of palaeo-sedimentary environment on oil yield: a case from Chang 7 oil layer of Triassic Yanchang Formation in southern Ordos Basin. *ActaGeochim.* 37, 228–243.
- Li, H., Liu, B., Liu, X., Meng, L., Cheng, L. and Wang, H., (2019):** Mineralogy and inorganic geochemistry of the Es4 shales of the Damintun Sag, northeast of the Bohai Bay Basin: implication for depositional environment. *Mar. Pet. Geol.* 110, 886–900.
- Li, T.-J., Huang, Z.-L., Chen, X., Li, X.-N. and Liu, J.-T., (2021):** Paleoenvironment and organic matter enrichment of the Carboniferous volcanic-related source rocks in the Malang Sag, Santanghu Basin, NW China. *Pet. Sci.* 18, 29–53.
- Li, X., Gang, W., Yao, J., Gao, G., Wang, C., Li, J., Liu, Y., Guo, Y. and Yang, S., (2020):** Major and trace elements as indicators for organic matter enrichment of marine carbonate rocks: A case study of Ordovician subsalt marine formations in the central-eastern Ordos Basin, North China. *Mar. Pet. Geol.* 111, 461–475.
- Long, X., Yuan, C., Sun, M., Xiao, W., Wang, Y., Cai, K., Jiang, Y., (2012).** Geochemistry and Nd isotopic composition of the Early Paleozoic flysch sequence in the Chinese Altai, Central Asia: evidence for a northward-derived mafic source and insight into Nd model ages in accretionary orogen. *Gondwana Res.* 22, 554–566.
- McLennan, S.M., Taylor, S.R., McCulloch, M.T. and Maynard, J.B., (1990):** Geochemical and Nd-Sr Isotopic Composition of Deep Sea Turbidites: Crustal Evolution and plate Tectonic Association. *Geochemical et Cosmochimica Acts*, 54, 2015-2050.
- McLennan, S.M., Hemming, S., McDaniel, D.K., Hanson, G.N. 1993. Geochemical approach to sedimentation, provenance, and tectonics. In: Johnson, M.J., Basu, A. (eds.), *Processes Controlling the Composition of Clastic Sediments: Geological Society of America, Special Paper* 284, 21-40
- Moradi, A.V., Sarı, A. and Akkaya, P., (2016):** Geochemistry of the Miocene oil shale (Hançili Formation) in the Çankırı-Çorum Basin, Central Turkey: Implications for Paleoclimate conditions, source–area weathering, provenance and tectonic setting *Sediment. Geol.* 341, 289–303.
- Nton, M.E and Otoha, O.W., (2011).** Lithofacies and Organic Geochemical studies of Akinside 1582 well, Eastern Dahomey Basin, Southwestern Nigeria. *Nigerian Association of Petroleum Explorationist Bulletin*, Vol. No. 23, No. 1, 107-117.
- Nton, M.E. and Adeyemi, M.O., (2014):** Petrography, compositional characteristic and stable isotope geochemistry of the Ewekoro Formation from Ibese Corehole, eastern Dahomey Basin, southwestern Nigeria. *Global Journal of Geological Sciences* Vol. 13, pg. 35-52
- Nton, M.E. Ezech, F.P. and Elueze, A.A. (2006):** Aspects of source rock evaluation and diagenetic history of the Akinbo Shale, eastern Dahomey Basin, southwestern Nigeria. *Nigerian Association of Petroleum Explorationists Bulletin*, Vol. 19, No. 1, 35-48,
- Obaje, N. G. (2009):** *Geology and Mineral Resources of Nigeria* (221 p). Berlin: Springer.<https://doi.org/10.1007/978-3-540-92685-6>

**Ogbe, F.G.A. (1972):** Stratigraphy of Strata Exposed in Ewekoro Quarry, Western Nigeria. In: Dessauvage, T.F.J. and Whiteman, A.J., Eds., African Geology, University of Ibadan Press, Ibadan, 305-322.

**Okosun, E.A. (1990):** A review of the Cretaceous stratigraphy of the Dahomey Embayment, West Africa. *Cretaceous Res* 11(1): 17-27

**Okosun, E.A. (1998)** Review of the Early Tertiary Stratigraphy of Southwestern Nigeria. *Journal of Mining and Geology*, 34, 27-35.

**Olabode, S.O. (2006):** Siliciclastic Slope Deposits from the Cretaceous Abeokuta Group, Dahomey (Benin) Basin, Southwestern Nigeria. *Journal of African Earth Sciences*, 46, 187-200. <http://dx.doi.org/10.1016/j.jafrearsci.2006.04.008>

**Omatsola, M.E., Adegoke, O.S., (1981):** Tectonic evolution and Cretaceous stratigraphy of the Dahomey basin. *J. Min. Geol.* 8, 30–137.

**Onuoha, K.M. and Ofoegbu, C.O., (1988).** Subsidence and evolution of Nigeria's continental margin: implications of data from Afowo-1 well. *Mar. Petrol. Geol.* 5, 175–181.

**De Matos, D. and Renato, M., (2000):** Tectonic evolution of the equatorial South Atlantic. In: *Atlantic Rifts and Continental Margins*. American Geophysical Union. *Geophys. Monogr. Ser.*, v. 115, p. 331 - 354.

**Overare, B., Osokpor, J., Ekeh, P.C. and Azmy, K., (2020).** Demystifying provenance signatures and paleo-depositional environment of mudrocks in parts of south-eastern Nigeria: Constraints from geochemistry. *J. Afr. Earth Sci.* 172, 103954. doi: 10.1016/j.jafrearsci.2020.103954

**Pehlivanli, B.Y., (2019):** Factors controlling the paleo-sedimentary conditions of Çeltek oil shale, Sorgun-Yozgat/Turkey. *Maden Tetkik ve Arama Dergisi* 158, 251–263.

**Reyment R (1965):** Aspects of the Geology of Nigeria, University of Ibadan Press, p 144

**Rimmer, S.M., (2004):** Geochemical paleoredox indicators in Devonian–Mississippian black shales, Central Appalachian Basin (USA). *Chem. Geol. Geochem. Organic-Rich Shales: New Perspect.* 206, 373–391. <https://doi.org/10.1016/j.chemgeo.2003.12.029>.

Roser, B.P. and Korsch, R.J. (1986). Determination of tectonic setting of sandstone mudstone suites using SiO<sub>2</sub> content and K<sub>2</sub>O/Na<sub>2</sub>O ratio. *Jour. Geol.* 94, 635–650

**Schenau, S.J., Reichart, G.J. and De Lange, G.J., (2005):** Phosphorus burial as a function of paleoproductivity. *Geochim. Cosmochim. Acta* 69, 919–931.

**Schoepfer, S.D., Shen, J., Wei, H., Tyson, R.V., Ingall, E. and Algeo, T.J., (2015):** Total organic carbon, organic phosphorus, and biogenic barium fluxes as proxies for paleomarine productivity. *Earth Sci. Rev.* 149, 23–52.

**Slanky, M., (1962):** Contribution a l'étude géologique du bassin sédimentaire côtier au Dahomey et au Togo: Bureau des Recherches géologiques et minières, Mémoire 11, 270p.

**Song, Y., Li, S. and Hu, S., (2019):** Warm–humid paleoclimate control of salinized lacustrine organic–rich shale deposition in the Oligocene Hetaoyuan Formation of the Biyang Depression, East China. *Int. J. Coal Geol.* 202, 69–84.

- Tao, S., Xu, Y., Tang, D., Xu, H., Li, S., Chen, S., Liu, W., Cui, Y. and Gou, M., (2017):** Geochemistry of the Shitoumei oil shale in the Santanghu Basin, Northwest China: Implications for paleoclimate conditions, weathering, provenance and tectonic setting. *Int. J. Coal Geol.* 184, 42–56.
- Taylor, S.R. and McLennan, S.M. (1985):** The continental crust: its composition and evolution. Blackwell, London, p 312.
- Teng, G.E., (2004):** The distribution of elements, carbon and oxygen isotopes on marine strata and environmental correlation between them and hydrocarbon source rocks formation - An example from Ordovician Basin, China. PhD Dissertation. Graduate School of Chinese Academy of Sciences (Lanzhou Institute of Geology), Lanzhou (in Chinese)
- Teng, G.E., Liu, W.H., Xu, Y.C. and Chen, J.F., (2005):** Correlative study on parameters of inorganic geochemistry and hydrocarbon source rocks formative environment. *Adv. Earth Science* 20, 193–200.
- Tribovillard, N., Algeo, T.J., Lyons, T. and Riboulleau, A., (2006):** Trace metals as paleoredox and paleoproductivity proxies: an update. *Chem. Geol.* 232, 12–32.
- Turekian, K.K. and Wedepohl, K.H. (1961):** Distribution of elements in some major units of earth's crust. *Geological Society of America Bulletin*, 72, 175–192.
- Wei, W. and Algeo, T.J., (2020):** Elemental proxies for paleosalinity analysis of ancient shales and mudrocks. *Geochim. Cosmochim. Acta* 287, 341–366.
- Wei, Y., Li, Xiaoyan, Zhang, R., Li, Xiaodong, Lu, S., Qiu, Y., Jiang, T., Gao, Y., Zhao, T. and Song, Z., (2021):** Influence of a paleosedimentary environment on shale oil enrichment: a case study on the Shahejie Formation of Raoyang Sag, Bohai Bay Basin, China. *Front. Earth Sci.* 9, 736054 <https://doi.org/10.3389/feart.2021.736054>.
- Whiteman, A. J. (1982):** Nigeria Its petroleum geology, resources and potentials. (1) 176, (2) 238. Graham and Trotman, London, U.K.
- Wronkiewicz, D.J. and Condie, K.C., (1990):** Geochemistry and mineralogy of sediments from the Ventersdorp and Transvaal Supergroups, South Africa: Cratonic evolution during the early Proterozoic *Geochimica et Cosmochimica Acta*, 54, 343–354.
- Xu, J., Liu, Z., Bechtel, A., Meng, Q., Sun, P., Jia, J., Cheng, L. and Song, Y., (2015):** Basin evolution and oil shale deposition during Upper Cretaceous in the Songliao basin (NE China): implications from sequence stratigraphy and geochemistry. *Int. J. Coal Geol.* 149, 9–23.
- Xu, Z., Lu, H., Zhao, C., Wang, X., Su, Z., Wang, Z., Liu, H., Wang, L. and Lu, Q., (2011):** Composition, origin and weathering process of surface sediment in Kumtagh Desert, Northwest China. *J. Geogr. Sci.* 21, 1062–1076.
- You, J., Liu, Y., Zhou, D., Zheng, Q., Vasichenko, K., and Chen, Z., (2020):** Activity of hydrothermal fluid at the bottom of a lake and its influence on the development of high-quality source rocks: Triassic Yanchang Formation, southern Ordos Basin, China. *Aust. J. Earth Sci.* 67, 115–128.

**Zhang, K., Liu, R., Liu, Z., Li, L., Wu, X. and Zhao, K., (2020):** Influence of palaeoclimate and hydrothermal activity on organic matter accumulation in lacustrine black shales from the Lower Cretaceous Bayingebi Formation of the Yin'e Basin, China. *Palaeogeogr. Palaeoclimatol. Palaeoecol.* 560, 110007 <https://doi.org/10.1016/j.palaeo.2020.11.0007>.

**Zhang, L., Dong, D., Qiu, Z., Wu, C., Zhang, Q., Wang, Y., Liu, D., Deng, Z., Zhou, S., Pan, S., (2021):** Sedimentology and geochemistry of Carboniferous-Permian marine- continental transitional shales in the eastern Ordos Basin, North China. *Palaeogeogr. Palaeoclimatol. Palaeoecol.* 571, 110389.

**Zhang, L., Xiao, D., Lu, Shuangfang, Jiang, S., Lu, Shudong, (2019):** Effect of sedimentary environment on the formation of organic-rich marine shale: Insights from major/trace elements and shale composition. *Int. J. Coal Geol.* 204, 34–50.

**Zhao, B.S., Li, R.X., Wang, X.Z., Wu, X.Y., Wang, N., Qin, X.L., Cheng, J.H. and Li, J.J., (2016):** Sedimentary environment and preservation conditions of organic matter analysis of Shanxi formation mud shale in Yanchang exploration area, Ordos Basin. *Geol. Sci. Technol. Inform.* 35, 109–117.

**Zheng, R. and Liu, H., (1999):** Study on palaeosalinity of Chang-6 oil reservoir set in Ordos Basin. *Oil Gas Geol.* 20, 20–25.

**Zhong, D.K., Jiang, Z.K., Guo, Q. and Sun, H.T., (2015):** A review about research history, situation and prospects of hydrothermal sedimentation. *J. Palaeogeogr.* 17, 285–296